The possible detection of OBrO in the stratosphere

Jean-Baptiste Renard, Michel Pirre, C Robert, Daniel Huguenin

▶ **To cite this version:**

HAL Id: insu-02879280

https://insu.hal.science/insu-02879280

Submitted on 23 Jun 2020

The possible detection of OBrO in the stratosphere

Jean-Baptiste Renard, Michel Pirre,[1] Claude Robert

Laboratoire de Physique et Chimie de l'Environnement / CNRS, Orléans, France

Daniel Huguenin

Geneva Observatory, Sauverny, Switzerland

Abstract. The analysis of spectral residua recorded at night by the balloon-borne AMON (Absorption par Minoritaires Ozone et Nox) UV-visible spectrometer during five stratospheric flights at middle and high latitudes shows that some absorption features remain in the 475 - 550 nm range, while the Rayleigh, aerosol, ozone, and NO_2 contributions are subtracted. The data reduction relating to these spectral lines is presented for the flight of February 26, 1997, at Kiruna (Sweden) inside the polar vortex. A good agreement exists between these unknown absorption features and those attributed to OBrO during recent laboratory measurements. The results of measurements from the other AMON flights are also presented. Assuming a OBrO cross section maximum similar to that of OClO, an upper limit for the OBrO mixing ratio is found to be around 20 pptv at midlatitude, implying that OBrO would be the principal bromine species at night in the middle stratosphere. At high latitude the OBrO mixing ratio decreases, particularly in the presence of OClO (also measured by AMON). The results are contradictory to current knowledge and, if confirmed, could argue for major revision of the assumed bromine chemistry in the stratosphere.

1. Introduction

Bromine species play an important role in stratospheric chemistry because they are involved in catalytic reactions leading to ozone depletion. Although much less abundant than chlorine species, they are expected to be of a more active form, which explains their importance in ozone chemistry, particularly inside the polar vortex.

Of the bromine family, only BrO and HBr have been detected by in situ and/or remote stratospheric measurements. Based on measurements of organic bromine at the tropopause [*Schauffler et al.*, 1993], total inorganic bromine (hereafter noted BrOy) is expected to maximize at 20 pptv in the stratosphere. BrO has been shown to range from 4 to 15 pptv in the daytime, with mixing ratios increasing with altitude, which is in good agreement with models [*Garcia and Solomon*, 1994]. An upper limit of a few pptv has been measured for HBr; this low mixing ratio confirms the partitioning in the bromine family in favor of the active species [*Traub et al.*, 1992; *Johnson et al.*, 1995]. Similarly, an upper limit for HOBr mixing ratios of a few pptv has been reported by *Johnson et al.* [1995]. Laboratory studies and modeling calculations [*Poulet et al.*, 1992] suggest that $BrONO_2$ and HOBr are the major species during the night, except in the polar vortex where the NO_2 mixing ratio is reduced and where BrCl would then constitute the major species. Although $BrONO_2$ and BrCl have not yet been detected in the stratosphere, measurements of BrO and OClO at sunset and sunrise [e.g., *Solomon et al.*, 1987, 1989; *Arpag et al.*, 1994] and measurements of OClO at night [*Renard et al.*, 1997a] are in agreement with modeling studies and could imply that the partitioning of the bromine species at night is well understood.

Some discrepancies nevertheless exist between observations and modeling studies, for example, the presence of BrO at night observed once by *Wahner et al.* [1990] inside the polar vortex. Although this measurement has not been confirmed and needs further study, it could indicate that the understanding of bromine chemistry is in fact incomplete.

During a laboratory study of the bromine-sensitized decomposition of ozone, a series of absorption bands were observed at a resolution of 0.6 nm in the 400 - 600 nm wavelength domain with a maximum absorption near 505 nm. These bands have been assigned to the bromine species OBrO [*Rattigan et al.*, 1994]. In the stratosphere this species could be formed as a minor channel of BrO + O_3 and BrO + ClO reactions, although it is generally accepted that its formation in nonnegligible amounts is unlikely (M. Chipperfield, personal communication, 1997). Tentative nighttime measurements of OBrO in the stratosphere have been carried out using the AMON (Absorption par Minoritaires Ozone et Nox) instrument and, surprisingly, high mixing ratios seem to be detected. This paper presents the experimental evidence of this detection. We will first describe in detail the AMON

---

[1] Also at Université d'Orléans, Orléans, France.

instrument and the data reduction, and then discuss the results and some consequences for the bromine chemistry.

2. Method of Observation

2.1. The AMON Instrument

All stratospheric gas species that present spectral features in the visible domain can be detected at night by the balloon-borne UV-visible spectrometer AMON provided that their spectral signature have an optical depth greater than 10^{-3}. This instrument, which has operated in the northern hemisphere since 1992, is essentially dedicated to the observation of O_3, NO_2, and NO_3 at middle and high latitudes, but has also enabled the establishment of the first vertical profile of OClO at night inside the polar vortex [*Renard et al.*, 1997a].

AMON, which uses stars as light source, is composed of a 20-cm telescope, a grating spectrometer, and a charge-coupled device (CCD) detector of 578 x 385 pixels [*Naudet et al.*, 1994]. The UV-visible domain is covered by five spectral bands: 350 - 400 nm, 400 - 475 nm, 475 - 550 nm, 550 - 625 nm, and 625 - 700 nm. The star spectrum is divided into these bands by using dichroic mirrors. Because of the nonlinear transmission, and particularly the weak transmission at the edges of the domains, it is impossible to retrieve a calibrated star spectrum and thus a continuous cover of the visible wavelength domain. Studies of atmospheric absorption features are then performed separately in these 50-nm and 75-nm length bands.

2.2. Stellar Occultation Method

AMON performs observations using the stellar occultation method, the principle of which is given below. Details of data reduction are presented in section 3.

The stellar occultation method consists in analyzing modifications caused by atmospheric species in the spectrum of a setting star (the path length of the light of sight is roughly 200 km for a tangent layer 1 km thick). First, a reference spectrum is recorded while the star is a few degrees above the gondola horizon and the balloon is at its float altitude. Spectra are then recorded while the star is below the balloon horizon, with an exposure time between 20 and 50 s (selected depending on the global level of the signal to optimize the response of the detector). These spectra are divided by the reference spectrum to remove the stellar absorption lines, the only remaining features being the signature of the stratospheric species. A least squares fit is applied to each spectrum to retrieve the slant column densities using the cross sections of the species. Finally, the vertical profiles of the species are obtained by using the "onion peeling" method.

Five AMON flights have taken place since 1992, three from the midlatitude Aire sur l'Adour (France) launching base (May 24, 1992, at 0100 UT, October 16, 1993, at 0050 LT, and March 24, 1994, at 2230 LT), and two from the high-latitude Kiruna/Esrange base (Sweden, Arctic polar circle) inside the polar vortex (February 10, 1995, at 2330 UT, and February 26, 1997, at 2200 UT). The last flight was performed during the validation campaign of the Improved Limb Atmospheric Spectrometer (ILAS) instrument on board the Advanced

Earth Observing Satellite (ADEOS). The float altitude of the balloon was 39 km, 39 km, 34 km, 32 km, and 32 km, respectively. During these flights the stars used for the observations were Regulus (α Leo), Altair (α Aquila), Rigel (β Orionis), Sirius (α Canis Major), and Rigel again, respectively. Observation conditions have made it possible to obtain lines of sight with minimum altitudes in the ranges 25 - 39 km, 18 - 39 km, 20 - 32 km, 14 - 30 km, and 13 - 32 km, respectively.

2.3. Theoretical Performances of the CCD Detector of AMON

The theoretical characteristics and performance of the CCD detector (CCD 2220 imaging system of Astromed), cooled at -132°C, are described by *Robert* [1992]. The readout noise is five electrons rms, and the photon noise reduces the signal-to-noise ratio to values close to 1000 per pixel. To minimize the noise and the effect of the individual response of the pixels, spectra are enlarged on the CCD onto strips of 10 pixels width perpendicular to dispersion, using a cylindrical lens. The strips on each band are added together during data reduction to produce the star spectra. The stray light contamination, measured on strips of five pixels width on both sides of the star spectra, is then subtracted. The spectra are sampled to 0.18 nm and 0.14 nm per pixel (parallel to dispersion) in the UV and visible domains, respectively. In practice the spectra are smoothed over at least five pixels, which gives a minimal spectral resolution of 0.9 nm and 0.7 nm in the UV and visible domains, respectively (this resolution is suitable for NO_2 retrieval and for other species with larger absorption lines). Consequently, each value of the spectra results from an average of at least 5 x 10 = 50 pixels of the CCD, and noise is reduced by a factor around of 7 (square root of 50). Thus, during the occultation, spectral structures greater than $1/(7 \times 1000)$, that is, 0.15×10^{-3}, are theoretically detectable with a signal-to-noise ratio of 1.

2.4. Real Detector Performances

During real observations in the stratosphere, OClO measurements performed by AMON on February 10, 1995, inside the polar vortex [*Renard et al.*, 1997a] have shown that absorption features of about $\pm 5 \times 10^{-3}$ can be detected in the 350 - 400 nm band, at least with the star (Sirius) used that time, which exhibits a strong UV spectrum. An example showing the good agreement between an AMON spectrum in this band and the OClO fit is presented on Figure 1a (standard deviation between the observed spectrum and the fit is 3×10^{-3}). In the 475 - 550 nm band, which is the band of interest for OBrO detection, the intensity of the star spectra reaches a maximum, as does the sensitivity of the CCD. We have computed that the signal recorded by AMON in this band is five times higher than in the UV band. Thus, absorption features of $\pm 10^{-3}$ are really observable in this spectral domain with a signal-to-noise ratio greater than 1.

Nevertheless, noise from the individual response of the pixels could lead to a bias in the detection of small absorption features. To test the possibility of such an artifact, we can reconsider the OClO retrieval, by searching for OClO in the measurements performed at
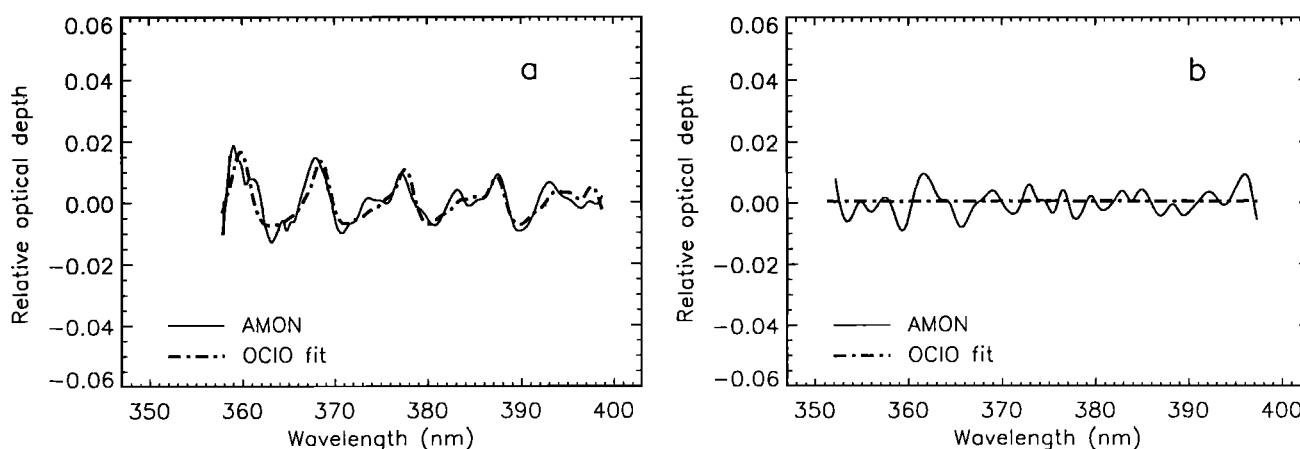
Figure 1. (a) Example of an observed UV spectrum (smoothed over 15 pixels parallel to dispersion) for the flight at Kiruna on February 10, 1995, and comparison with a least squares fit using OClO cross sections. Balloon altitude is 30 km, and star elevation is -3.4°. The OClO retrieval shows the ability of AMON to detect small absorption features. (b) Example of an observed UV spectrum for the flight at Aire sur l'Adour on March, 24, 1994, and comparison with an OClO fit. Balloon altitude is 34 km, and star elevation is -2.3°. This spectrum corresponds to noise, and no OClO is detected.

midlatitude. By applying the OClO data reduction procedure described by *Renard et al.* [1997a] to the data obtained during the 1994 flight, we obtain slant column densities in the $\pm$ 5×10^{14} cm^{-2} range, with an average value near zero. This value implies OClO mixing ratios of 0 $\pm$ 5 pptv, which agrees with present knowledge of this species at midlatitude (this test was not conducted for the 1992 and 1993 flights because the signal on the UV band is too weak). Figure 1b presents an example of a spectrum for the 1994 flight and the OClO fit; standard deviation is 4×10^{-3}. Since no OClO is detected, this value corresponds to noise and is similar to that obtained for the 1995 flight.

Thus, the good quality fit when OClO is present and the zero detection when no OClO is expected confirm that no bias is induced by the detector in the UV band (and it seems reasonable to extend this result to the other spectral bands of AMON).

2.5. Pointing System

During stratospheric flight, the spectrometer is mounted on the stabilized platform of the Geneva Observatory [*Huguenin*, 1994], which is equipped with a pointing system with an accuracy of 3 arc sec rms. High-precision spectra are obtained when variations of the balloon float altitude are small (typically below $\pm$ 100 m), when the pointing system is as accurate as expected and when no depointing problems occur due to strong stratospheric winds.

For the 1992 and 1993 AMON flights, the signal-to-noise ratio was not maximal because the stars were not bright enough and pointing was not optimized. During the 1994 and 1995 flights, depointing problems were encountered at the beginning of the occultation which prevented the recording of excellent reference spectra (they are usable, but slightly noisy). Furthermore, some spectra were lost during the first half of the occultation. For the 1997 flight the pointing system had been improved, and the very high stability of the stabilized platform made it possible to maximize the signal-to-noise ratio and

increase the ability of the spectrometer to detect small absorption features. A high-quality reference spectrum has been obtained by averaging 17 consecutive spectra (Figure 2). Data reduction to retrieve atmospheric species will thus be presented using the 100 spectra recorded during this flight.

3. Atmospheric Species Retrieval

3.1. Ozone and NO₂ Data Reduction

Data reduction for O$_3$, NO$_2$, and OClO, and for the resultant vertical profiles, is described by *Renard et al.* [1996, 1997a, b]. In brief, dark current is subtracted, cosmic ray traces removed, and the scale adjusted on the H and He lines of the star. Retrieval of the NO$_2$, O$_3$ and OClO slant column is performed where their absorption lines are stronger, in the 410 - 470 nm domain, the Chappuis bands in the 550 - 625 nm domain, and the 355 - 400 nm domain, respectively. A sliding average procedure over five consecutive spectra is applied to all spectra in order to decrease the effect of the chromatic scintillation (induced by the motion of air masses along the line of sight). The spectra are then smoothed by a Gaussian filter over 5, 30, and 15 pixels, respectively, in order to match the spectral features in the respective domains (see, for example, *Roscoe et al.* [1996] discussion concerning the smoothing procedure applied to the NO$_2$ retrieval). The signal residua, after subtracting all the other absorbents (including Rayleigh scattering), are attributed to the contribution of aerosol. Since the work of *Renard et al.* [1996, 1997a, b], improvements have been made concerning the data reduction procedure. In particular, analysis of the absorption lines on the AMON spectra is now performed using larger spectral windows (i.e., 75 nm instead of 65 nm for O$_3$, 60 nm instead of 30 nm for NO$_2$, 45 nm instead of 35 nm for OClO). Following the application of this new procedure to the 1993, 1994, and 1995 data, some differences in the results were observed, mainly where the signal-to-noise ratio of
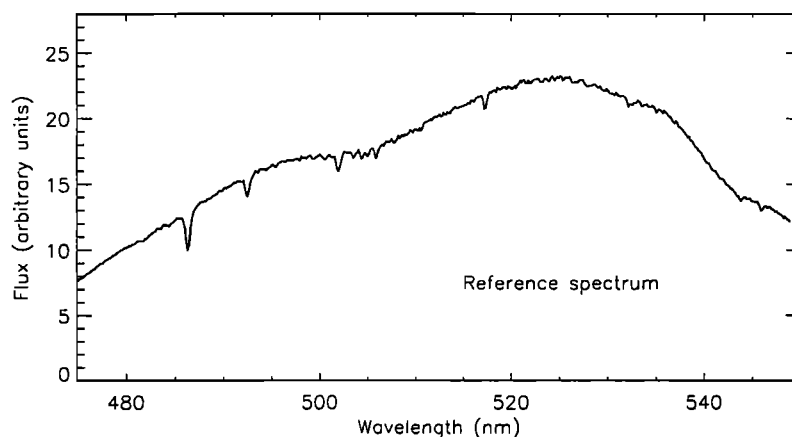
Figure 2. Reference spectrum (raw data) in the AMON 475 - 550 nm spectral band for the flight at Kiruna (Sweden, Arctic polar circle) on February 26, 1997. The shape of the Rigel (β Orionis) spectrum is modified according to the response of the CCD and the nonlinear transmission of a dichroic mirror in the optical system of AMON. The main absorption lines on the spectra are attributed to H (at 486 nm), He (at 492 nm and 502 nm), and Mg (at 517 nm).

the spectra is low (typically below 2). Nevertheless, the discrepancy between the slant column density data using the old and the new versions is less than 20%.

For the 1997 flight data, Figure 3 presents an example of the observed spectra of O_3 and NO_2 and the fit obtained using a least squares method and the Reims University cross sections of ozone (J. Brion, personal communication, 1997) and NO_2 [*Coquart et al.*, 1995]. The standard deviation is equal to 1.5×10^{-3} and 2.5×10^{-3}, respectively. The slant column profiles obtained for O_3 and NO_2 are presented in Figure 4.

3.2. The 475 - 550 nm Spectral Band

The main contributions in the 475 - 550 nm band are O_3 and NO_2 (Figure 5a). Their removal, which uses their slant column densities previously obtained (Figure 4), involves a careful examination of their cross sections to prevent introducing artificial features. We have compared the NO_2 cross sections of *Schneider et al.* [1987] to those

of *Coquart et al.* [1995] (below 500 nm) and those measured recently by the Global Ozone Monitoring Experiment (GOME) instrument (A. Dehn and A. Richter, personal communication, 1997). No significant discrepancies exist concerning the position of the absorption features for the various data sets in this spectral domain. Recently, *Harder et al.* [1997] measured the NO_2 cross sections at 294 K, 239 K, 230 K, and 217 K and concluded that no measurable temperature-dependent wavelength shift exists. A temperature decrease only increases the values of the differential cross sections, with variations in a 10 - 40 % range. These measurements give confidence concerning the precision of the position of the absorption lines in this spectral domain.

We have also compared the O_3 cross sections of Reims University (J. Brion, personal communication, 1997) to those of GOME (A. Dehn and A. Richter, personal communication, 1997); these are the two most recent data sets available at high spectral resolution in this wavelength domain. Some discrepancies appear in the
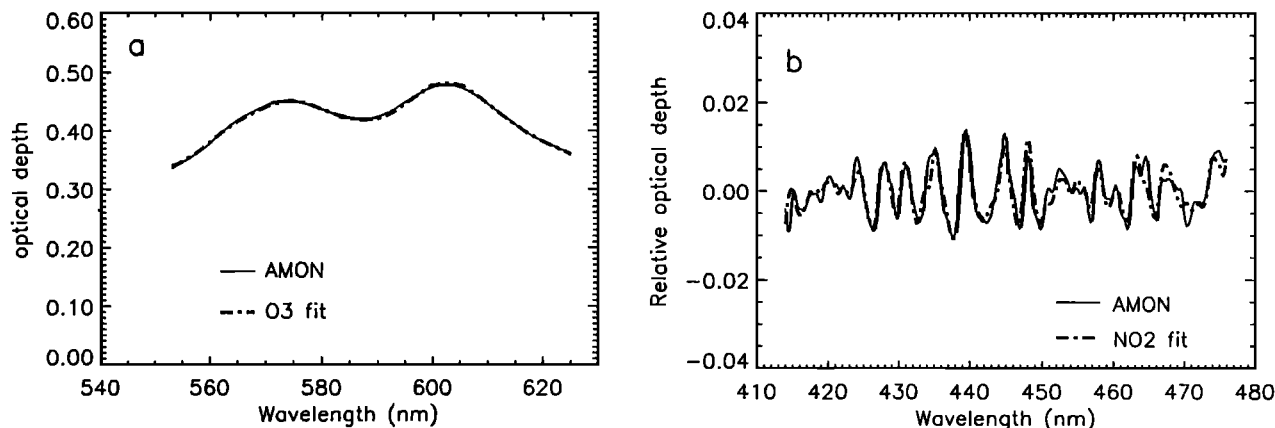
Figure 3. Example of observed spectra of (a) O_3 and (b) NO_2 for the 1997 flight. Balloon altitude is 32 km, and star elevation is -2.0°, which corresponds to a line of sight with a tangent height of 28 km. The data are smoothed over 30 pixels and five pixels respectively.

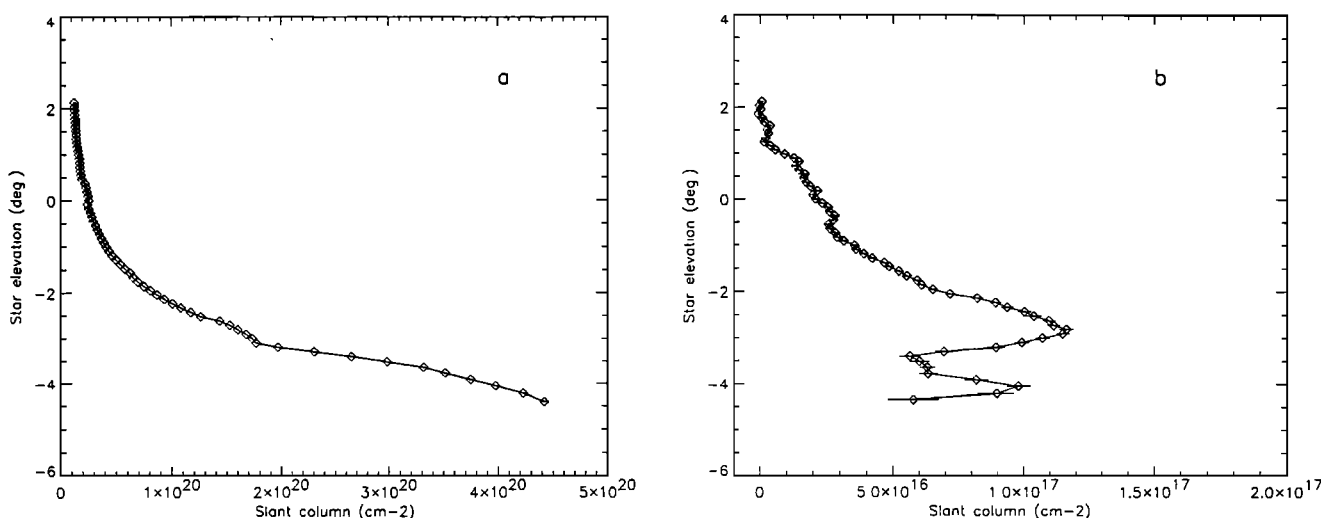**Figure 4.** Slant column profiles of (a) O_3 and (b) NO_2 for the 1997 flight.

shape of the small absorption features, and their position is shifted by at least 0.4 nm (although the Reims University data perfectly match the AMON spectra in the 550 - 625 nm domain, i.e., at the maximum of the Chappuis bands). After discussing this with the above mentioned authors, it seems that these discrepancies result from an unexpected temperature dependence in the Chappuis bands, and that they are located at the sensitivity detection limit of the instrument used during the laboratory measurements. However, since these small features are larger than those of NO_2 (and OBrO), this problem only implies undulation in the general trend of the spectra and can be minimized by using the mathematical high-pass filter described below.

The spectra are smoothed by a Gaussian filter on 15 pixels. The reference spectrum and the cross sections used in the 475 - 550 nm domain are similarly smoothed. After subtracting the O_3 and NO_2 contributions (Figures 5b and 5c), a high-band pass filter is applied to all spectra (Figure 5d). This filter consists of a Fourier transformer on which the seven first frequencies are discarded to remove the aerosol and Rayleigh contributions, the effect of chromatic scintillation, and the ozone residua, respectively. The band pass of the filter was selected to optimize the fitting procedure without significantly altering the shape of the cross section absorption lines. This same so-called differential method was also applied for NO_2 and OClO retrieval. Finally, some unknown absorption features remain permanently at the same place in all the AMON spectra between 475 and 550 nm, regardless of which NO_2 and ozone cross sections are used. In the following, the GOME cross sections will be used for NO_2 and the Reims University cross sections for ozone (for homogeneity with data reduction on other AMON's spectral bands).

3.3. OBrO Detection

The remaining features can be fitted using the cross sections attributed to OBrO by *Rattigan et al.* [1994]. Figure 6 presents four spectra obtained for the 1997 flight and the OBrO fit. The star elevation was +1.5° for the first spectra, and no OBrO seems to be present (Figure

6a). The standard deviation between the spectrum and the fit is 0.2×10^{-3}, which corresponds to the noise when the recorded stellar flux is at its maximum. Because of the set of the star, the flux decreases for the other spectra, and thus the noise increases. For the other three spectra on Figure 6 (with a star elevation of respectively -1.4°, -2.0°, and -2.3°), the standard deviation is 0.5×10^{-3}, 0.6×10^{-3} and 1.0×10^{-3}, respectively, and the signal-to-noise ratio (here computed by the ratio of the fit maximum amplitude to the standard deviation) is 2.9, 4.0, and 3.1, respectively.

Almost all the peaks have a good fit, although some small discrepancies remain around 500 nm and 515 nm, and around 485 nm for low lines of sight. They may originate from small residua of the main stellar lines H at 486 nm, and He at 492 nm and 502 nm, and of the Mg line at 517 nm (these lines are represented in Figure 2), but could also be a consequence of the uncertainties in the OBrO small absorption features, since these cross sections were measured at ambient temperature and could be slightly different at low temperature.

No absolute values of the OBrO cross sections are presently available. To derive values of slant column density, we assume that the maximum at 505 nm is similar to that of OClO, that is, $1.5 \times 10^{-17} \text{ cm}^2$. This value has also been estimated by *Miller et al.* [1997]. Figure 7 presents the evolution of OBrO slant column density versus star elevation. If we compare bromine-containing species with chlorine-containing analogues in the UV-visible domain, the cross sections for the bromine species are invariably larger. This would imply that the column densities in Figure 7 probably represent an upper limit.

3.4. Interference With Other Species

We must consider the possibility that the structures attributed here to OBrO exist in the ozone cross sections, but have not yet been measured. These structures would correspond to variations of 1% in the cross sections, which is smaller than the noise in the Reims and GOME data. We assume that the existence of such small ozone structures is unlikely because they would occur at the
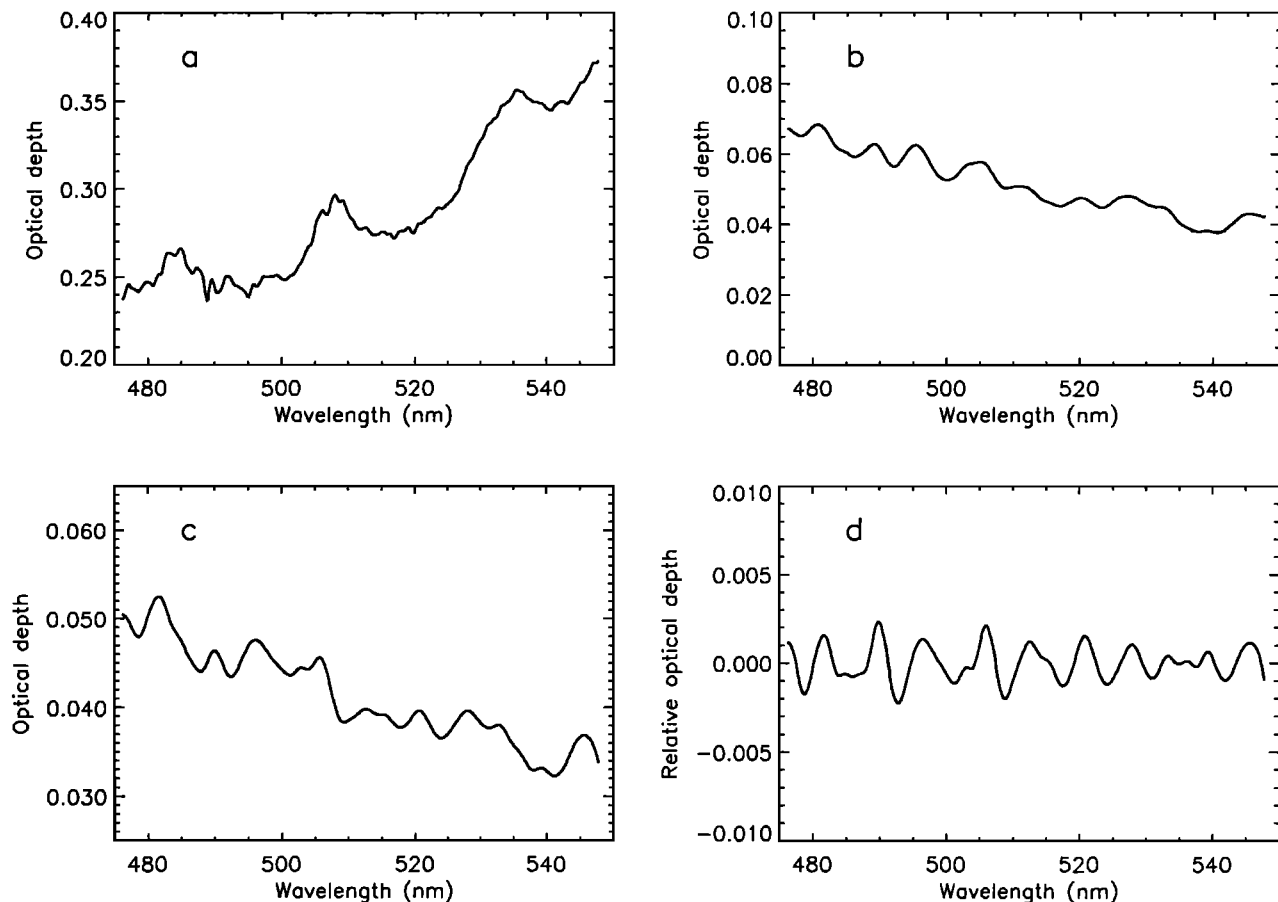
Figure 5. Optical depth in the 475 - 550 wavelength domain for the 1997 flight (star elevation is - 2.0°). (a) Raw spectrum smoothed over five pixels. (b) Spectrum (smoothed over 15 pixels) obtained after subtracting the ozone and Rayleigh contributions. (c) Spectrum obtained after subtracting the NO_2 contribution (the remaining slope is due to the aerosol and chromatic scintillation contributions). (d) Spectrum after applying the high-pass filter.

same place as the OBrO lines, although high-accuracy measurements of ozone cross sections are necessary to confirm our assumption.

Other contamination could originate from uncertainties in the NO_2 cross sections. But the structures we attribute to OBrO would correspond to a 10% variation in NO_2 cross sections, which seems unlikely. Another contamination could originate from a shift in the wavelength scale of NO_2 cross sections. Figure 8 presents the evolution of the signal-to-noise ratio of the OBrO retrieval if we shift the NO_2 cross sections up to ± 2 nm, for a spectrum recorded with a star elevation of -2.0°. The signal-to-noise ratio remains above 3 for a shift of ± 0.5 nm, which shows that the retrieval is not very sensitive to small errors in the wavelength scale. Greater error seems improbable because these cross sections were measured by various teams and are in excellent agreement.

Since the temperature varies by a few tens of Kelvins along the line of sight, we have also examined the influence of the temperature-dependent NO_2 cross sections on the retrieval (with no shift on the absorption lines, as discussed previously). One test consisted in retrieving the NO_2 slant column profiles in the 400 - 475 nm band using the *Harder et al,* [1997] data at 217 K, 230 K, 239 K, and 294 K, and then subtracting the different optical

depths (i.e., cross sections at a given temperature multiplied by the slant column densities obtained at the same temperature) from the 475 - 550 nm spectra. It appears that the resultant four new OBrO slant column profiles vary by less than 7%. Another test consisted in computing the OBrO retrieval with an NO_2 optical depth smaller and greater by 20 per cent than its value at 217 K, in order to simulate the maximum variation that occurs for some of the NO_2 lines. Again, the slant column profile of OBrO changes by less than 8% (which is in the error bars of the retrieval), while both the signal-to-noise ratio and the correlation of the fit decrease. Thus, the method used for the OBrO retrieval does not appear to be very sensitive to the temperature-dependent NO_2 cross sections.

Noise can contaminate the smoothing procedure for low lines of sight where the signal-to-noise ratio is close to 1. To test the sensitivity of the retrieval to the smoothing procedure, different widths between five and 15 pixels were used for the Gaussian filter (a smoothing on more than 15 pixels, i.e., 2 nm, would alter the shape of the OBrO cross sections). Taking into account the uncertainties due to the error bars, we found that the slant column profiles obtained with the various smoothing are similar. The values resulting from our data reduction are thus not distorted by noise.
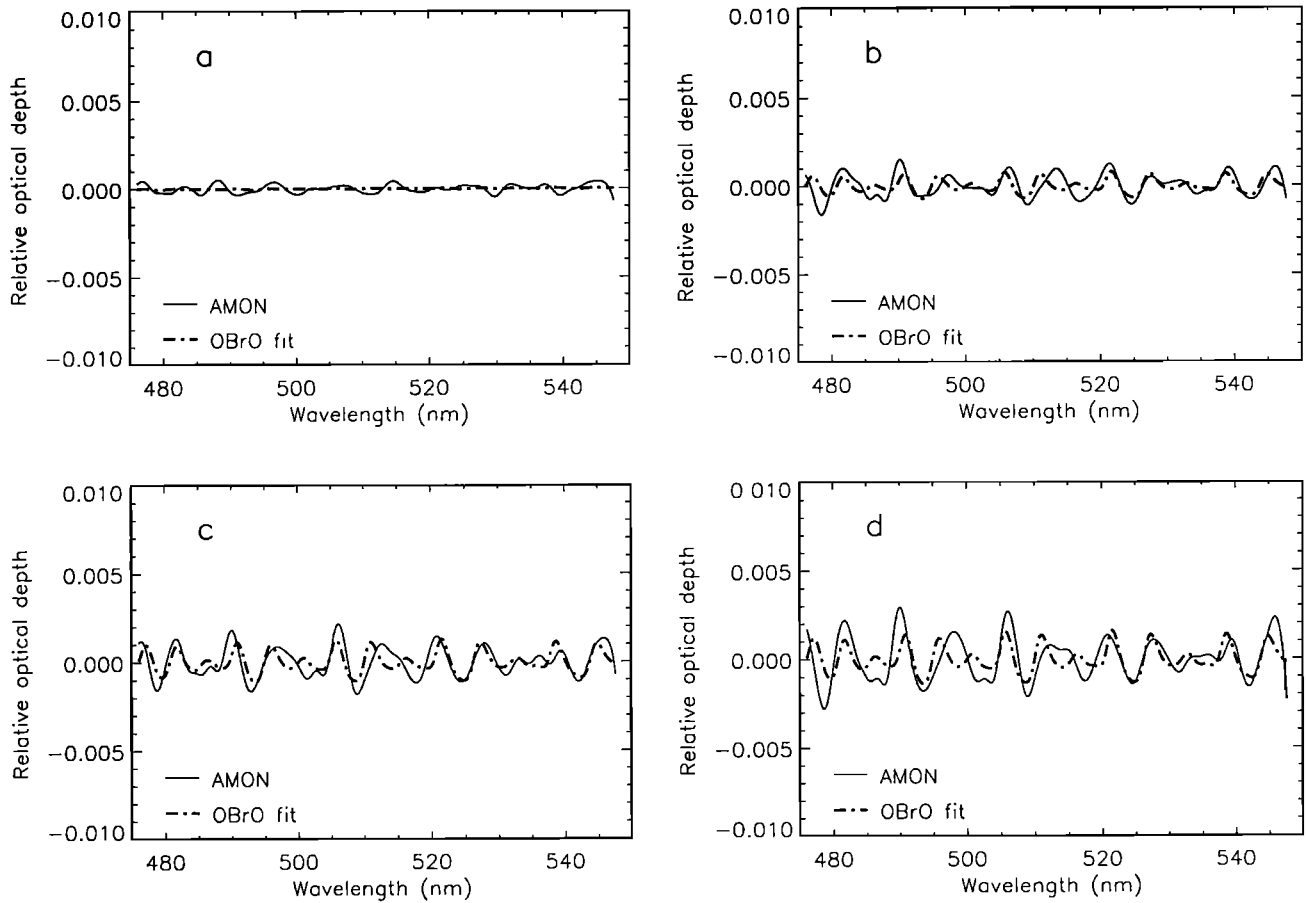
Figure 6. Spectra residua for the 1997 flight after subtracting the O_3 and NO_2 contributions, and after removing the Rayleigh, aerosol, scintillation, and the ozone residua contributions using a high-pass filter. A comparison is shown with a fit using the OBrO cross sections. The data are smoothed over 15 pixels. The star elevation was (a) +1.5°, (b) -1.4°, (c) -2.0°, and (d) -2.3°. The first spectrum corresponds to noise obtained at maximum transmission. The signal-to-noise ratio for the three other spectra is 2.9, 4.0, and 3.1, respectively.
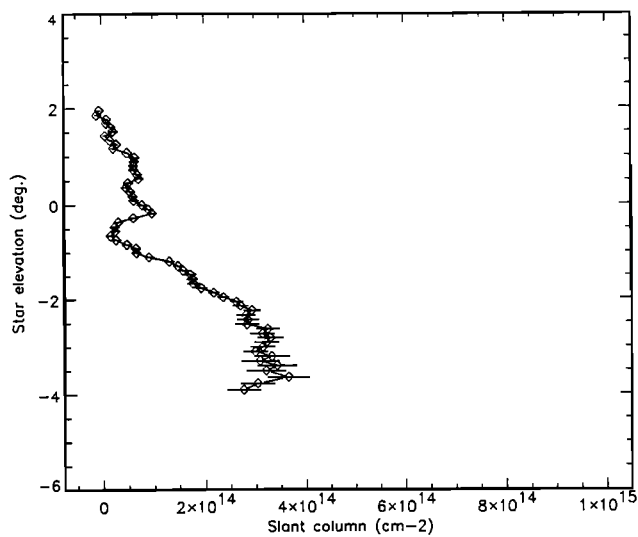
Figure 7. OBrO slant column densities versus star elevation for the 1997 flight.
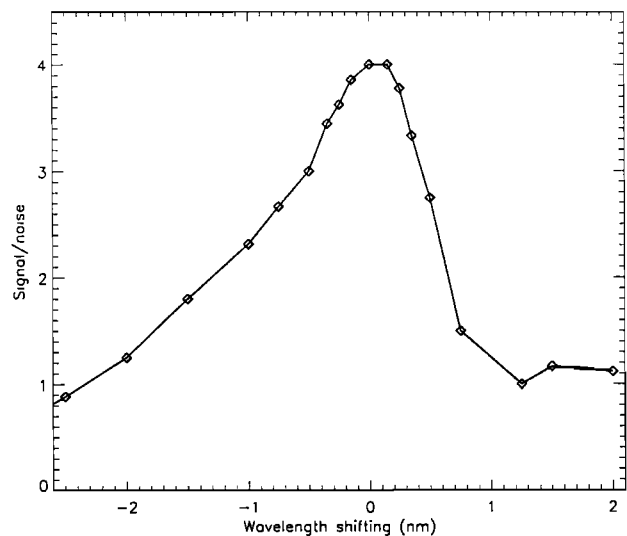
Figure 8. Influence of shifting the wavelength scale of NO_2 cross sections, using the signal-to-noise ratio obtained during the OBrO retrieval for a spectrum recorded with a star elevation of -2.0°.

Finally, it is noted that the OBrO slant column profile is relatively smooth and that no negative values exist. This profile is quite different from those of O_3 and those of NO_2, at least in the polar vortex, which also suggests that the structures we attribute to OBrO are probably not due to contamination by other species.

In conclusion, the tests performed at the various steps of data reduction indicate that some unknown absorption features have probably been detected by AMON. The best current candidate for this signature is OBrO.

3.5. Other AMON Flights

The new absorption lines around 500 nm can be searched for using the data acquired during the other flights of AMON. Because data quality is lower than for the 1997 flight (due to the flight conditions, as explained above), the residua of the main stellar lines cannot be totally removed. Nevertheless, the absorption features detected on the 1997 flight remain at the same place as for the 1993 and 1994 flights, though different stars were used and the spectra did not have the same location on the CCD. Figure 9 presents an example of four spectra for the 1993 flight. The standard deviations are between 0.4×10^{-3} and 1.1×10^{-3}, and the signal-to-noise ratio reaches 4.8 for the two last spectra. These values are greater than for the

1997 flight because higher slant column densities of OBrO are detected. Figure 10 presents an example of four spectra recorded during the 1994 flight. Because of the poor quality reference spectrum, the best signal-to-noise ratio is only around 3. For the 1992 and 1995 flights the spectra are more noisy, and only a statistic detection can be performed. Figure 11 presents the slant column profiles obtained for the first four flights of AMON.

4. Results and Discussion

Vertical profiles are obtained using the "onion peeling" method. The slant column profiles are slightly smoothed before inversion to avoid oscillations in the resultant profiles. Some mathematical improvements have also been made to the inversion method since the work of Renard et al. [1996, 1997a, b]. By comparison with these published results, we have smoother profiles, an increase in the NO_2 mixing ratios below 20 hPa for the 1993 flight, and a better sampled OClO profile for the 1995 flight.

The 1997 profiles have been compared to other measurements performed on the same date and at similar locations (also as part of the ILAS validation campaign). A very good agreement exists between the AMON O_3 profile and the ozone-sounding measurements, and also
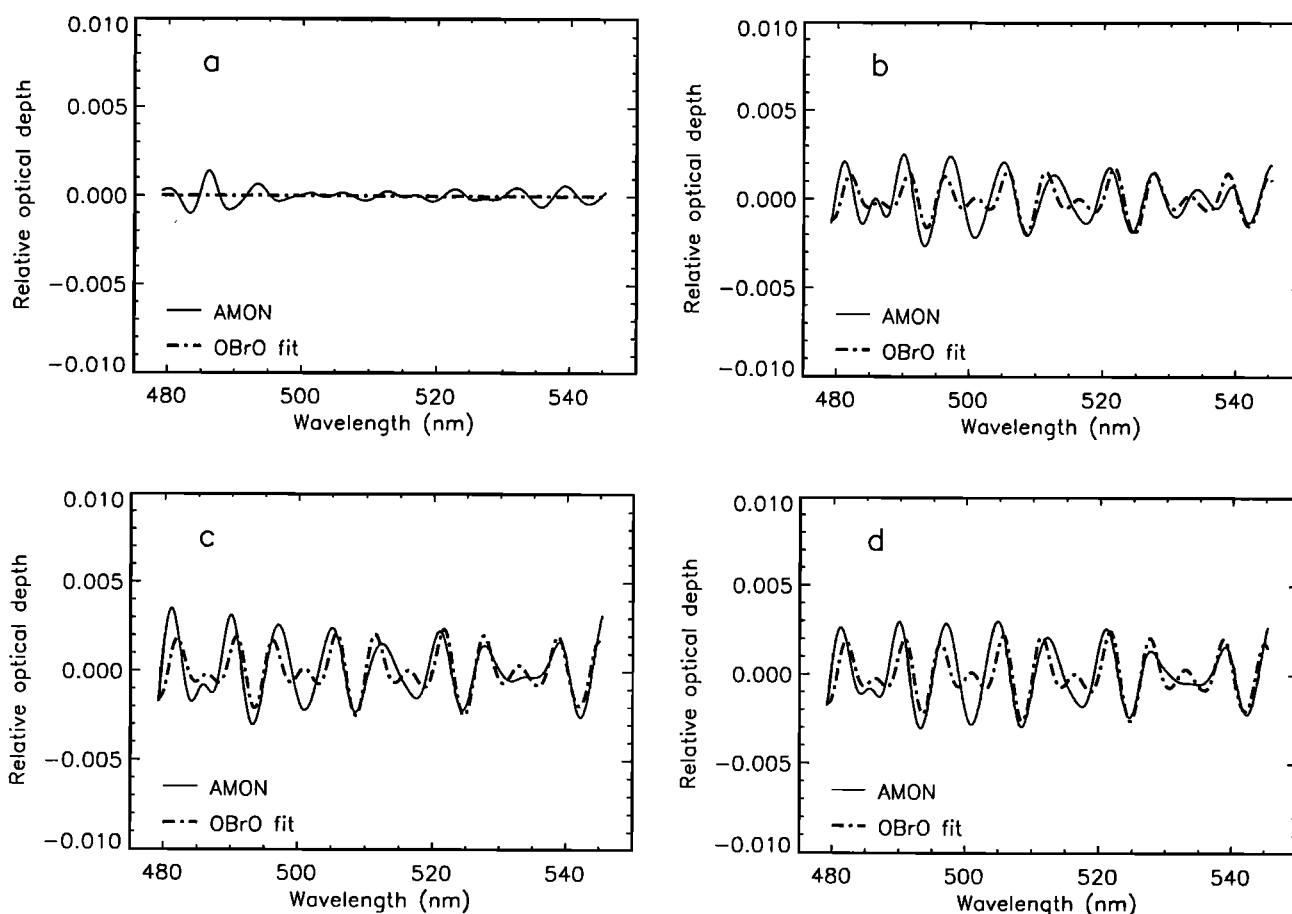
Figure 9. Spectra for the midlatitude flight at Aire sur l'Adour (France) on October, 16, 1993. The star elevation was (a) +1.5°, (b) -3.3°, (c) -3.5 degree, and (d) -3.8°. The first spectrum, obtained at maximum transmission, corresponds to noise. The signal-to-noise ratio for the three other spectra is 4.2, 4.8, and 4.8, respectively.
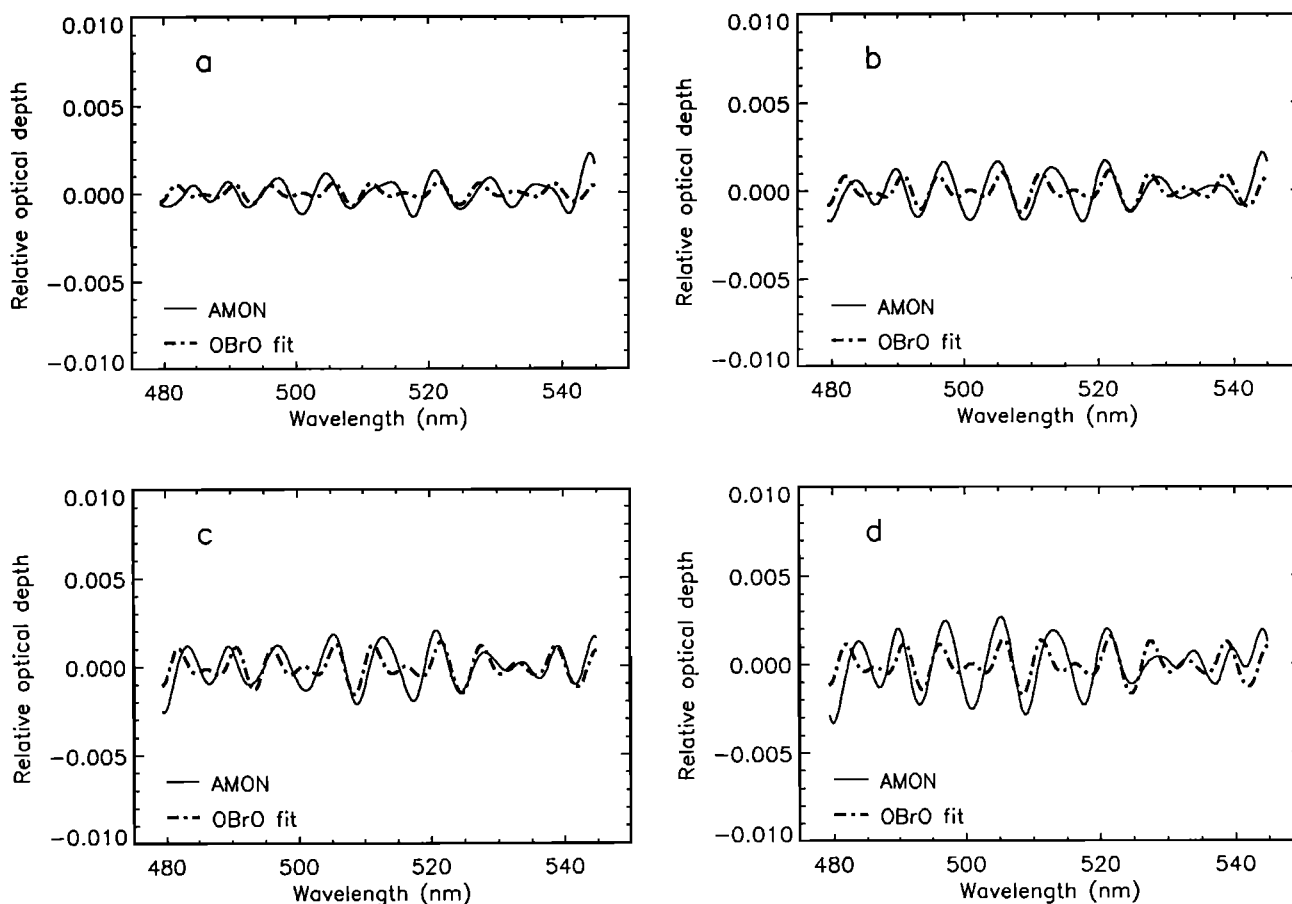
Figure 10. Spectra for the midlatitude flight at Aire sur l'Adour (France) on March, 24, 1994. The star elevation was (a) -1.7°, (b) -2.0°, (c), -2.3 degree, and (d) -2.8°. Because of the poor quality reference spectrum, the best signal-to-noise ratio is only around 3.

between the AMON NO₂ profile and the two profiles obtained at sunset by the Limb Profile Monitor of the Atmosphere (LPMA) instrument (C. Camy-Peyret, personal communication, 1997), taking into account the small difference in the location of the measurements and after correcting for the diurnal variation. This result provides good confidence in the AMON data reduction procedure.

Figure 12 presents the set of OBrO profiles obtained with AMON. The three profiles obtained at midlatitude are close together and totally different from the two profiles obtained at high latitude. As stated previously, these values must be considered as upper limits.

Figure 13 presents, after converting the profile to mixing ratio versus pressure, the OBrO profile of the 1993 flight and a comparison with the NO₂ and extinction coefficient of aerosol profiles. The upper limit for OBrO mixing ratios is in the 20-25 pptv range. If the estimation of *Schauffler et al.* [1993] for BrOy is correct, our results seem to indicate that OBrO could be the major bromine species at night in a large part of the stratosphere at midlatitude. OBrO mixing ratios would be high even in the presence of a high NO₂ mixing ratio (these two species have constant mixing ratios in the middle stratosphere, while their profiles differ in the lower stratosphere). Thus, the reaction which could generate OBrO would have to compete with the fast reaction

$$BrO + NO_2 + M \longrightarrow BrONO_2$$

which is commonly accepted to take place in the stratosphere. Moreover, this new reaction would most likely have to operate in the gaseous phase because OBrO is detectable even when the aerosol extinction coefficient is very low, as shown in Figure 13.

Figure 14 presents the profiles obtained during the 1997 flight in mixing ratio versus pressure. At high latitude in winter inside the polar vortex, where NO₂ mixing ratios are low, it seems that OBrO mixing ratios decrease when OClO is present. Thus, the formation of OClO, correlated with the decrease of NO₂ mixing ratios, seems to prevent the generation of a large amount of OBrO.

To date, no instruments have been able to detect BrONO₂ and BrCl, which implies that we cannot check the modeling concerning bromine chemistry at night. As mentioned before, the nighttime detection of BrO in the vortex by *Wahner et al.* [1990] could indicate that modeling studies are incomplete. Some adjustments will be performed in the spectral domain of the UV band of AMON before the flight scheduled for February 1999 in the polar vortex, as part of the THESEO (Third European Stratospheric Experiment on Ozone) campaign, so as to cover the BrO spectral bands and confirm or reject this BrO detection. Thus, by also considering the
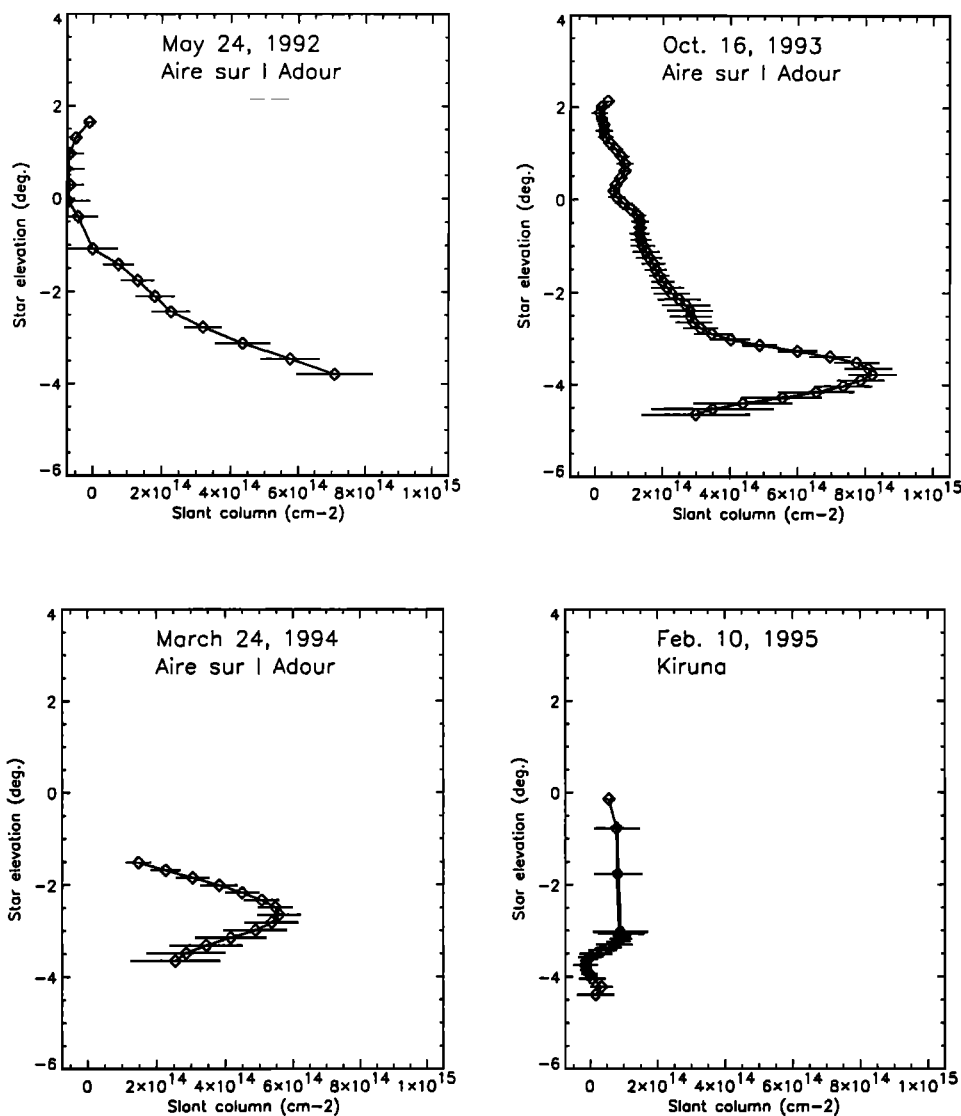
Figure 11. OBrO slant column profile versus star elevation for the first four flights of AMON. The profiles are slightly smoothed before inversion to avoid oscillations in the results.

measurements of OClO and probably of OBrO, the stellar occultation method in the UV-visible domain performed by AMON can significantly contribute to a better understanding of bromine partitioning in the stratosphere. Such measurements using the same method will be also performed by the Global Ozone Monitoring by Occultation of Stars (GOMOS) instrument on board the European ENVISAT satellite after 1999. GOMOS will perform a global coverage of the stratospheric trace species with absorption lines in the UV-visible domain and is potentially able to confirm the detection of OBrO.

5. Conclusion

The presence of the absorption bands assigned to OBrO in the AMON spectra could have important implications for bromine photochemistry, and therefore for the ozone depletion problem. Although we have demonstrated that systematic bias probably does not occur during the data

reduction, we cannot totally exclude the possibility that the permanent absorption features recorded by AMON could result from errors or uncertainties in the O_3 or NO_2 cross section measurements.

It is clear that other in situ or remote measurements are needed to confirm the presence of OBrO in the stratosphere. Laboratory studies are also required to determine the reactions leading to the formation of OBrO. In addition, absolute values of the OBrO cross sections at low temperature are urgently needed, which could eventually significantly modify our estimated OBrO mixing ratios. Values must preferably be obtained at a resolution below the 0.14 nm theoretical resolution of AMON in order to increase the quality of the fit for the small absorption features. Cross sections of NO_2 and O_3 at temperatures of 200 K or below are also needed to reproduce the conditions encountered in the polar vortex. Such improvements would make it possible to increase the feasibility of OBrO detection in the stratosphere.
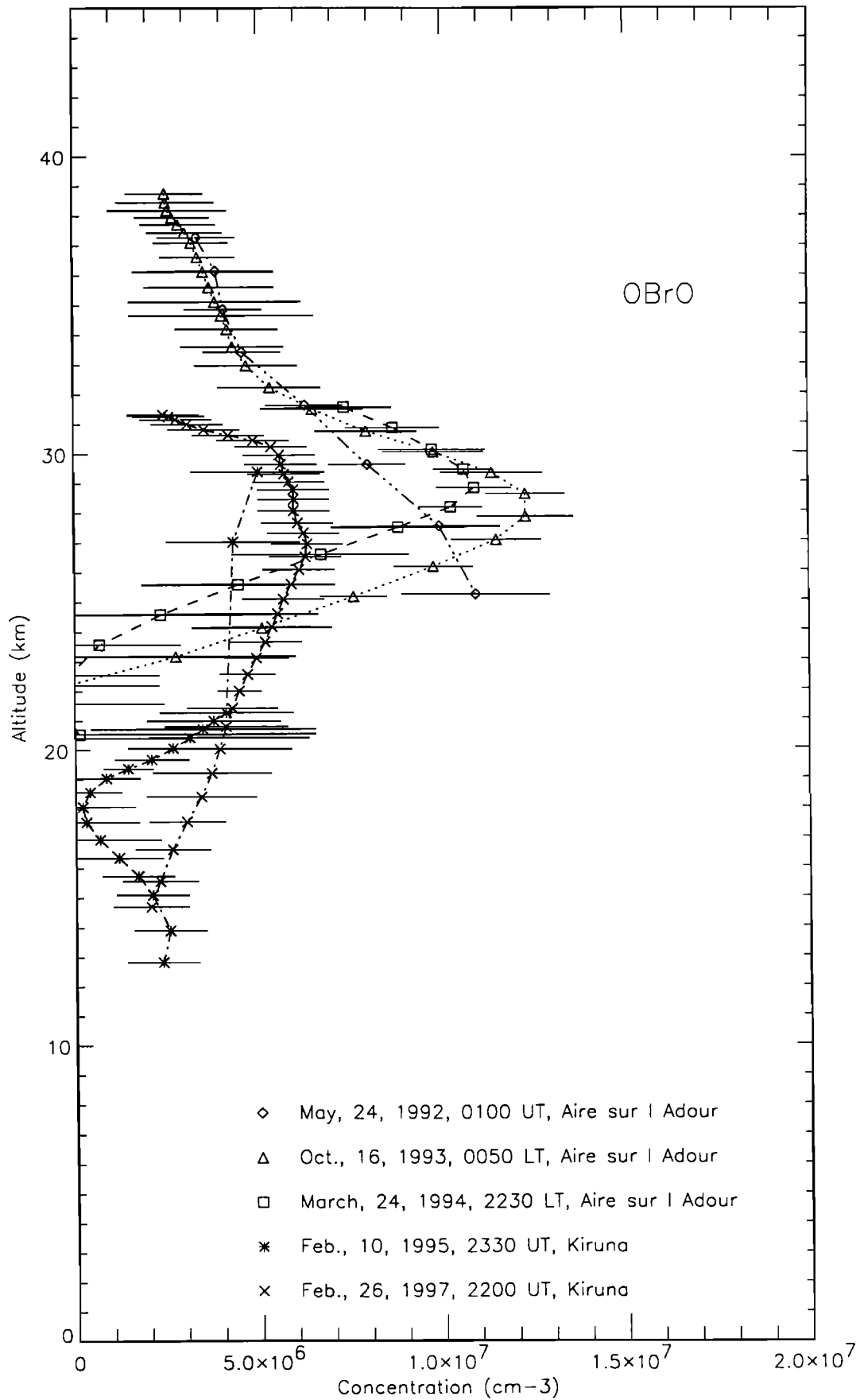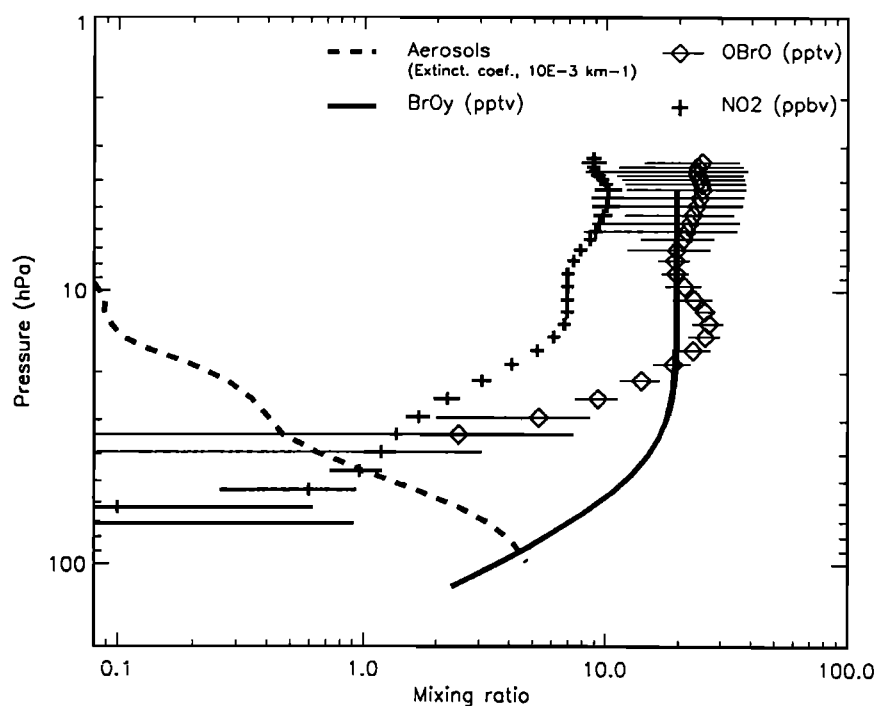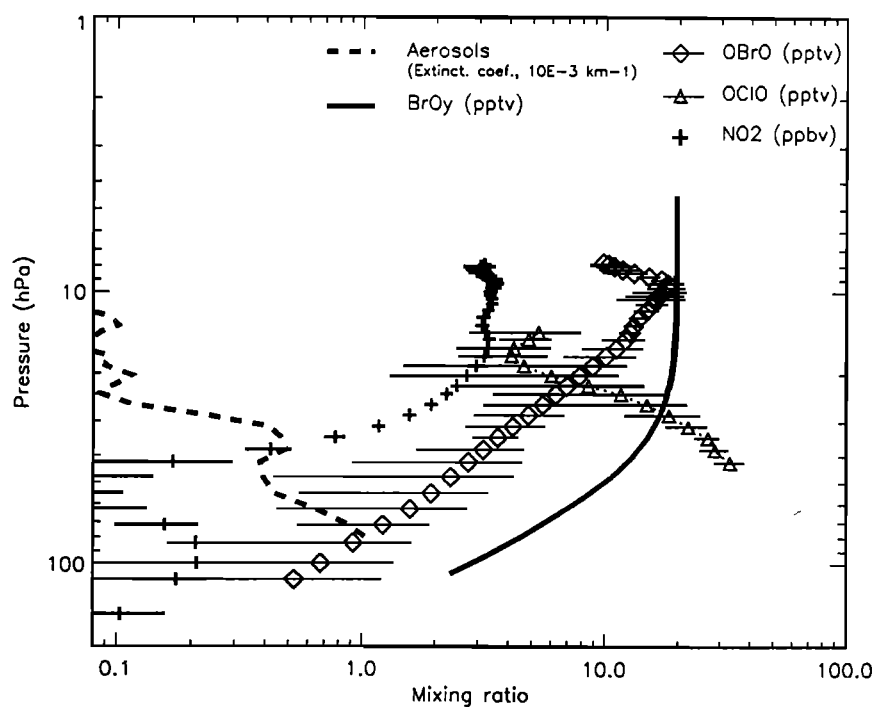
Figure 12. Vertical distribution of OBrO for the five flights of AMON.

Figure 13. OBrO vertical distribution and comparison with vertical distribution of NO_2, the extinction coefficient of aerosol (averaged on the 350 - 700 nm spectral domain), and total bromine species (BrOy) predicted by models, for the midlatitude flight on October 16, 1993. The OBrO cross sections are assumed to have a maximum of 1.5×10^{-17} cm^{-2}.

Figure 14. OBrO vertical distribution and comparison with vertical distribution of NO_2, OClO, the extinction coefficient of aerosol (averaged on the 350 - 700 nm spectral domain), and BrOy predicted by models, for the flight inside the polar vortex on February 26, 1997.

References

Arpag, K.A., P.V. Johnson, H.. Miller, R.W Sanders, and S. Solomon, Observations of the stratospheric BrO column over Colorado 40°N, *J. Geophys. Res.*, *99*, 8175-8181, 1994.

Coquart, B., A. Jenouvier, and M.F. Mérienne, The NO_2 absorption spectrum temperature effect in the wavelength region 400-500 nm, *J. Atmos. Chem.*, *21*, 251-261, 1995.

Garcia, R.R., and S. Solomon, A new numerical model of the middle atmosphere, 2., Ozone and related species, *J. Geophys. Res.*, *99*, 12937-12951, 1994.

Harder, J.W., J.W. Brault, P.V. Johnston, and G.H. Mount, Temperature dependent NO_2 cross sections at high spectral resolution, *J. Geophys. Res.*, *102*, 3861-3879, 1997.

Huguenin, D., Design and performance of stratospheric balloon-borne platforms for infrared astrophysical observations, *Infrared Phys. Technol.*, *35*(2/3), 195-202, 1994.

Johnson, D.G., W.A Taub, K.V. Chance, and K.W. Jucks, Detection of HBr and upper limit of HOBr: Bromine partitioning in the stratosphere, *Geophys. Res. Lett.*, *22*, 1373-1376, 1995.

Miller, E.C., S.L. Nickolaisen, J.S. Francisco, and S.P. Sander, The OBrO $C(^2A_2) < -- X(^2B_1)$ absorption spectrum, *J Chem. Phys.*, *107*(7), 2300-2307, 1997.

Naudet, J.P., C. Robert, and D. Huguenin, Balloon measurements of stratospheric trace species using a multichanel UV-Visible spectrometer, in *Proceedings of the 14th ESA Symposium on European Rocket and Balloon Programs and Related Research, ESA SP-355*, pp. 165-168, Eur. Space Agency, Paris, France, 1994.

Poulet, G., M. Pirre, F. Maguin, R. Ramaroson, and G. Le Bras, Role of the BrO + HO_2 reaction in the stratospheric chemistry of bromine, *Geophys. Res. Lett.*, *19*(23), 2305-2308, 1992.

Rattigan, O.V., R.L. Jones, and R.A. Cox, The visible spectrum of gaseous OBrO, *Chem. Phys. Lett.*, *230*, 121-126, 1994.

Renard, J.B., M. Pirre, C. Robert, G. Moreau, D. Huguenin, and J.M. Russell III, Nocturnal vertical distribution of stratospheric O_3, NO_2 and NO_3 from balloon measurements, *J. Geophys. Res.*, *101*, 28793-28804, 1996.

Renard, J.B., F. Lefèvre, M. Pirre, C. Robert, and D. Huguenin, Vertical profile of night-time stratospheric OClO, *J. Atmos. Chem.*, *26*, 65-76, 1997a.

Renard, J.B., M. Pirre, F. Lefevre, C. Robert, B. Nozière, E. Lateltin, and D. Huguenin, Vertical distribution of nighttime stratospheric NO_2 from balloon measurements - Comparison with models, *Geophys. Res. Lett.*, *24*, 73-76, 1997b.

Robert, C., Réalisation d'un spectromètre stellaire multicanal embarquale sous ballon stratosphérique, Ph.D. thesis, Univ. of Orléans, Orléans, France, 1992.

Roscoe, H.K., D.J. Fish, and R.L. Jones, Interpolation errors in UV-visible spectrometry for stratospheric sensing: Implications for sensivity, spectral resolution, and spectral range, *Appl. Opt.*, *35*, 427-432, 1996.

Schauffler, S.M., L.E. Heidt, W.H. Pollock, T.M. Gilpin, J.F. Vedder, S. Solomon, R.A. Lueb, and E.L. Atlas, Measurements of halogenated organic compounds near the tropical tropopause, *Geophys. Res. Lett.*, *20*, 2567-2570, 1993.

Schneider, W., G.K. Moortgat, G.S. Tyndall, and J.P. Burrows, Absorption cross sections of NO_2 in the UV and visible region (200 - 700 nm) at 298 K, *J. Photochem. Photobiol.*, *A*, *40*, 195-217, 1987.

Solomon, S., G.H. Mount, R.W. Sanders, and A.L. Schmeltekopf, Visible spectrometry at McMurdo station, Antarctica, 2., Observations of OClO, *J. Geophys. Res.*, *92*, 8329-8339, 1987.

Solomon, S., R.W. Sanders, M.A. Carroll, and A.L. Schmeltekopf, Visible and near-ultraviolet spectroscopy at McMurdo Station, Antarctica, 5., Observations of the diurnal variations of BrO and OClO, *J. Geophys. Res.*, *94*, 11393-11403, 1989.

Traub, W.A., D.G. Johnson, K.W. Jucks and K.V. Chance, Upper limit for stratospheric HBr using far-infrared thermal emission spectroscopy, *Geophys. Res. Lett.*, *19*, 1651-1654, 1992.

Wahner, A., J. Callies, H.P. Dorn, U. Platt, and C. Schiller, Near UV atmospheric absorption measurements of column abundance during Airborne Arctic Expedition, January-February 1989, 3., BrO Observations, *Geophys. Res. Lett.*, *17*, 517-520, 1990.

D. Huguenin, Observatoire de Genève, CH-1290 Sauverny, Switzerland.

M. Pirre, J.B. Renard and C. Robert, LPCE/CNRS, 3A Avenue de la Recherche Scientifique, F-45071 Orléans cedex 2, France. (e-mail: mpirre@cnrs-orleans.fr; jbrenard@cnrs-orleans.fr; clrobert@cnrs-orleans.fr).